

# Influence of oxygen on structure and optical properties of AZO films

D. GIRBOVAN, D. MARCONI, R. REDAC<sup>a</sup>, A. V. POP<sup>\*</sup>

*Babes-Bolyai University, Physics Faculty, M. Kogalniceanu No. 1, 400084, Cluj-Napoca, Romania,*

*<sup>a</sup>Aurel Vlaicu University, Faculty of Engineering, B-dul Revoluției nr. 77, 310130 Arad, România*

Aluminum-doped ZnO (AZO) films are deposited onto the glass substrate by RF magnetron sputtering method. The influence of oxygen concentration in flow sputtering gas on structure and optical properties of AZO are studied. The X-ray diffraction (XRD) shows that the films are highly oriented with their crystallographic *c*-axis perpendicular to the substrate and that the grain size is influenced by oxygen concentration. The AZO films have high optical transmission in the visible range. The decrease of bandgap energy  $E_g$  with increasing oxygen concentration in the flow sputtering gas is described by the Burstein-Moss effect.

(Received July 23, 2012; accepted September 20, 2012)

*Keywords:* Al-ZnO films, RF sputtering, XRD, Optical transmission

## 1. Introduction

Zinc Oxide (ZnO) is a II-VI n-type semiconductor with a wide band gap (3.3 eV at 300 K). The electrical conductivity and optical properties of doped ZnO makes this material attractive for transparent conducting films. Thus, n-type ZnO films have been successfully used in various applications as n-type layers in light-emitting diodes as well as transparent ohmic contacts. ZnO and doped ZnO:Al (AZO) thin films are used as superstrate configuration of tandem Si solar cell[1]. Compared with undoped ZnO, the Al-doped ZnO (AZO) films have a lower resistivity and better stability [2].

Several techniques have been used to fabricate epitaxial and textured ZnO and AZO films including molecular beam epitaxy, sputtering and pulsed-laser deposition (PLD)[3]. Among these techniques, R.F. magnetron sputtering is widely used in fabricating metal oxide thin films and related materials because of its low cost, simplicity and low operating temperature. Many reports already showed that the properties of AZO thin films were mainly influenced by processing parameters during sputtering, such as substrate temperature, discharge power, target-substrate distance and oxygen flow content [4-8].

The structural characteristics, electronic and optical properties of the AZO thin films as function of the oxygen pressure during deposition have been investigated widely [9-11]. In this paper we report on the growth and characterization of epitaxial AZO films on glass substrates, for transparent conducting electrodes in a solar cell application, by using different oxygen concentration in the flow sputtering gas. The structural and optical properties of the AZO films grown by R.F. magnetron sputtering were also characterized.

## 2. Experimental

The ZnO and Al doped ZnO thin films were deposited by RF magnetron sputtering technique. Ceramic circular targets with chemical compositions ZnO and  $\text{Al}_{0.02}\text{Zn}_{0.98}\text{O}_x$  (sample AZO) were obtained by solid state reaction method, using mechanical mixed powders of 99.99% pure ZnO and 99.97% pure  $\text{Al}_2\text{O}_3$ . The films were deposited on glass substrate by using the oxygen-argon atmosphere as sputtering gas. The deposition pressure in the chamber was  $2 \times 10^{-2}$  mbar and the target-to-substrate distance was 6 cm. The reactive gas is formed from Ar and  $\text{O}_2$  mixtures, having the mass flows  $d_{\text{Ar}}$  and  $d_{\text{O}_2}$ . The introduction of the reactive gas to the sputtering chamber was independently analysed using two mass flow controllers. The flux ratio  $f_{\text{O}_2} = d_{\text{O}_2} / (d_{\text{Ar}} + d_{\text{O}_2})$  used to characterize  $\text{O}_2$  concentration in the chamber, was in the range 0.00 to 0.75. The substrate temperature was 150°C. The films' thicknesses measured with the quartz monitor were around 900 nm.

The crystallinity of AZO films was investigated by X-ray diffraction (XRD) with Cr  $K_\alpha$  radiation.

Optical transmission measurements were done with a Carry 500 Spectrometer (300 nm – 1200 nm range).

From the transmission spectra, the optical constants were calculated using the program PARAV-V2.0. [12]. This program allowed to obtain the film thicknesses, the refractive index as a function of wavelength, the transmission and the absorption coefficient as a function of energy by fitting the Cauchy's dispersion formula. The dispersion of refractive index  $n$  is calculated from fringes data (experimentally observed peaks and valleys of  $T(\lambda)$  spectrum) in the fully transmitting region and the weak/medium absorption regions using Swanepoel's theory [12].

### 3. Results and discussion

X-ray diffraction patterns of the films prepared at different values of  $f_{O_2}$  are shown in Fig. 1. The films were polycrystalline and also show a preferential orientation in the (002) direction, the c-axis being perpendicular to the substrate [13, 14].

The lattice constant  $c$  of the samples increases from  $c=0.525$  nm for  $f_{O_2}=0$  to 0.527 nm when  $f_{O_2}$  is 0.75. When increasing the oxygen concentration in the sputtering gas, there is a change of the (002) diffraction peak linewidth, reflecting the variation of the mean grains' sizes.

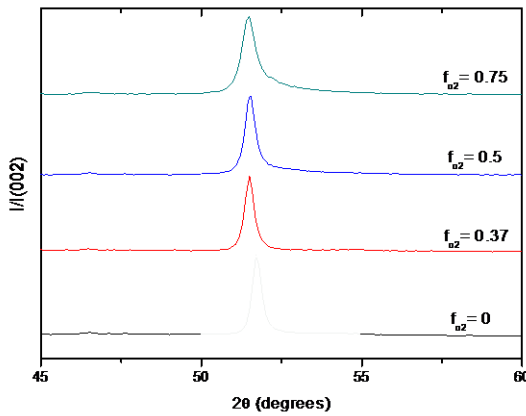


Fig. 1. XRD diffraction patterns of the films deposited at various flux ratios.

The crystallite sizes of the films were calculated using the Scherrer equation [8,15]. The mean grain size decreases from 42.3 nm to 26.2 nm when the oxygen ratio in the sputtering gas is increased from 0.00 to 0.75 (Table 1). The excess oxygen might induce defects in the films, which influenced the nucleation and growth of the films, and finally the degradation of the crystallinity in agreement with other results [7].

The optical transmission spectra of ZnO:Al films measured in the wavelength range  $\lambda=300-1200$  nm in air, at room temperature, is shown in Fig. 2. The average transmittance  $T(\lambda)$  of the films was around 83% in the visible region (from 500 nm to 1100 nm) with a sharp fall in the transmittance at the absorption edge around  $\lambda\sim 390$  nm.

Table 1. Variation of grain size  $D$ , optical bandgap  $E_g$  and film thickness  $d$ , versus the  $f_{O_2}$  ratio in sputtering gas of  $Zn_{0.98}Al_{0.02}O_x$  thin films.

$f_{O_2}$	0	0.375	0.5	0.75
$D$ (nm)	42.3	39.7	37.4	26.2
$E_g$ (eV)	3.47	3.42	3.37	3.35
$d$ (nm)	960	950	900	920

Similar results were reported for AZO films obtained by RF sputtering [14,15]. By increasing wavelength above

$\lambda\sim 500$  nm, the optical interference in AZO layers leads to oscillations in the transmittance. Both the minima and maxima values of the interference fringes increase when increasing the wavelength.

The insert of Fig. 2 shows the refractive index  $n(\lambda)$  calculated with PARAV-V2.0 program, for AZO film with  $f_{O_2} = 0.75$ . A decrease from  $n= 1.94$  to 1.915 with increasing wavelength from 400 nm to 1000 nm is shown. From the wavelength corresponding to two adjacent minima of  $\lambda_{m1}$  and  $\lambda_{m2}$ , the film thickness,  $d$  is estimated as:

$$d = \frac{\lambda_{m1} \cdot \lambda_{m2}}{2(n_1 \lambda_{m2} + n_2 \lambda_{m1})} \quad (1)$$

where  $n_2$  and  $n_1$  are the values of refractive index at wavelengths  $\lambda_{m2}$  and  $\lambda_{m1}$  respectively.

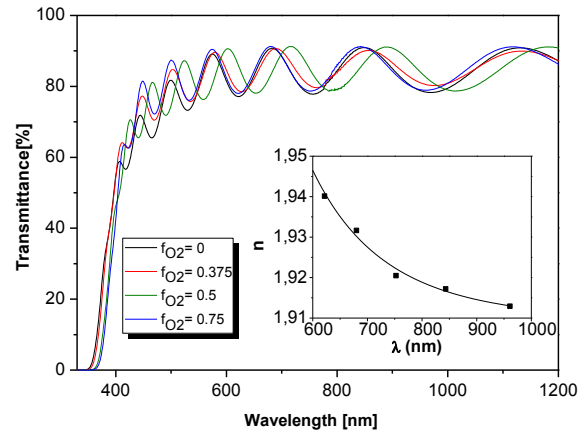


Fig. 2. Optical transmittance spectra of  $Zn_{0.98}Al_{0.02}O_x$  samples prepared with various  $O_2$  concentration in plasma. The insert shows the refractive index as a function of wavelength, for the film obtained using  $f_{O_2}=0.75$ . By solid line is the computed dependence with the second order polynomial law with PARAV program.

Table 1 shows that film thickness slowly decreases with the increase of oxygen content in sputtering gas. The bandgap energy,  $E_g$ , of ZnO layers is determined from the optical absorption coefficient  $\alpha(\lambda) = -\ln(T(\lambda))/d$ , which is calculated from measured transmission and layer thickness. The band gap,  $E_g$ , was determined according to the Tauc relation:

$$(\alpha h\nu)^2 = A^2(h\nu - E_g) \quad (2),$$

where  $\alpha$  is the absorption coefficient,  $A$  is a constant,  $h$  is Planck's constant,  $E_g$  is the optical bandgap.

Fig. 3 shows the Tauc plot of AZO films obtained for different content  $f_{O_2}$  of oxygen in sputtering gas and for ZnO film ( $f_{O_2}=0$ ), respectively. From linear fits to the data close to the absorption edge, the bandgap energy  $E_g$  is determined (Table 1). In the absence of oxygen in sputtering gas ( $f_{O_2}=0$ ) the optical energy gap is  $E_g=3.27$  eV for ZnO film and  $E_g = 3.47$  eV for AZO film. The increase of  $E_g$  after Al doping of ZnO is attributed to an increase in

the carrier concentration and the blocking of low energy transitions as predicted by Burstein-Moss theory [21]. For doped ZnO, the donor electrons occupy states at the bottom of the conduction band and the optical band gap is given by the energy difference between the states with Fermi momentum in the conduction and valence band. Similar behavior was reported previously in AZO films obtained by magnetron sputtering and PLD [16-20].

The optical gap of AZO film is influenced by the oxygen concentration in sputtering gas (Table 1). The band gap of  $Zn_{0.98}Al_{0.02}O_x$  thin films decreases from 3.47eV to 3.35eV, when  $f_{O_2}$  ratio increases from 0 to 0.75. Similar dependence was shown previously [7, 22]. The broadening of the optical band gap can be described by the relation

$$\Delta E_g = \left( \frac{\hbar^2}{2m_{cv}^*} \right) (3\pi^2 n)^{2/3} \quad (3)$$

where  $\Delta E_g$  is the band gap shift of the doped semiconductor with respect to the undoped one,  $m_{cv}^*$  the reduced effective mass,  $\hbar$  the Plank's constant and  $n$  is the carrier concentration, respectively [21].

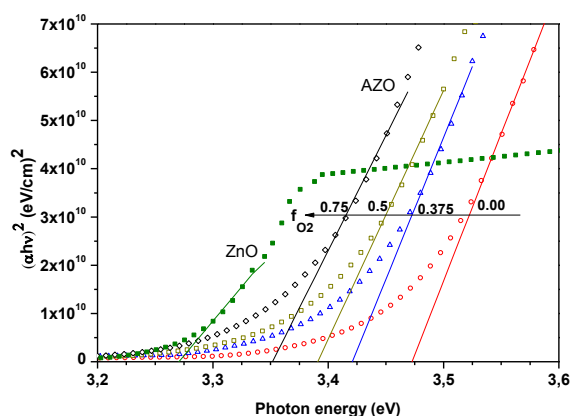


Fig. 3. Tauc plot for AZO thin films (obtained using  $0 \leq f_{O_2} \leq 0.75$ ) and ZnO thin film ( $f_{O_2}=0.375$ ).

The band gap decreases when decreasing carrier concentration. XRD shows that the crystallinity of the AZO films degraded with the increase of the oxygen content.

#### 4. Conclusions

High quality transparent doped ZnO thin films (AZO films) were grown using the RF sputtering technique on glass substrate starting from ZnO target containing 2 at.% of  $Al_2O_3$ . As the oxygen content in gas flow was increased, the linewidth of (002) diffraction peak was increased and a poorer crystallinity was shown.

The shift of the optical band gap of AZO films with increasing oxygen content in sputtering gas is due to a decrease in the carrier concentration, as described by

Burstein-Moss shift.

The increase of the oxygen content in sputtering gas had negative effects on the structural and optical properties of AZO films.

#### Acknowledgments

One of the authors (Dorina Girbovan) gratefully acknowledges the financial support within the POSDRU /88/1.5/S/60185 "INNOVATIVE DOCTORAL STUDIES IN A KNOWLEDGE BASED SOCIETY" Babeş-Bolyai University, Cluj-Napoca, Romania.

#### References

- [1] M. Zeman, Poortmans, J. & Arkhipov, V., John Wiley & Sons, 978-0-470-09126-5, New York, 173 (2007).
- [2] V. N. Zhitomirsky, E. Cetinorgu, E. Adler, Yu. Rosenberg, R. L. Boxman, S. Goldsmith, *Thin Solid Films* **515**, 885 (2006).
- [3] J. D. Pedarnig, J. Heitz, T. Stehrer, B. Praher, R. Viskup, K. Siraj, A. Moser, A. Vlad, M. A. Bodea, D. Bauerle, N. Hari Babu, D. A. Cardwell, *Spectrochim. Acta B* **63**, 1117 (2008).
- [4] Y. H. Kim, K. S. Lee, T. S. Lee, B. Cheong, T.-Y. Seong, W. M. Kim, *Appl. Surf. Sci.* **255**, 7251 (2009).
- [5] M. Chen, Z. L. Pei, C. Sun, J. Gong, R. F. Huang, L. S. Wen, *J. Mater. Sci. Eng. B.* **85**, 212 (2001).
- [6] S. Kobayakawa, Y. Tanaka, A. Ide-Ekessabi, *Nucl. Instr. Meth. Phys. Res. B.* **249**, 536 (2006).
- [7] Dong-Hyun Hwang, Jung-Hoon Ahn, Kwan-Nam Hui, Kwan-San Hui, Young-Guk Son, *J. Ceram. Proc. Res.* **12**, 150 (2011).
- [8] Dorina Girbovan, M. A. Bodea, D. Marconi, J. D. Pedarnig, A. Pop, *Studia UBB Chemia*, **LVI**, 213 (2011).
- [9] K. Ellmer, K. Diesner, R. Wendt and S. Fiechter, *Solid State Phenom.* **51-52**, 541 (1996).
- [10] S. Brehme, F. Fenske, W. Fuhs, E. Nebauer, M. Poschenrieder, B. Selle, I. Sieber, *Thin Solid Films* **342**, 163 (1999).
- [11] H. Sato, T. Minami, S. Takata, *Thin Solid Films* **220**, 327 (1992).
- [12] A. Ganjoo, R. Golovchak, *J. Optoelectron. Adv. Mater.* **10**, 1328 (2008).
- [13] H. T. Cao, Z. L. Pei, J. Gong, C. Sun, R. F. Huang, L. S. Wen, *Surf. Coat. Tech.* **184**, 84 (2004).
- [14] M. Suche, S. Christoulakis, N. Katsarakis, T. Kitsopoulos, G. Kiriakidis, *Thin Solid Films* **515**, 6562 (2007).
- [15] J. J. Ding, S. Y. Ma, H. X. Chen, X. F. Shi, T. T. Zhou, L. M. Mao, *Physica B* **404**, 2439 (2009).
- [16] Qing Hua Li, Deliang Zhu, Wenjun Liu, Yi Liu, Xiao Cui Ma, *Appl. Surf. Sci.* **254**, 2922 (2008).
- [17] E. L. Papadopoulou, M. Varda, K. Kouroupis-Agalou, M. Androulidaki, E. Chikoidze, P. Galtier, G. Huyberechts, E. Aperathitis, *Thin Solid Films* **516**, 8141 (2008).

- [18] W. Y. Zhang, D. K. He, Z. Z. Liu, L. J. Sun, Z. X. Fu, Optoelectron. Adv. Mater.- Rapid Commun. **4**, 1651 (2010).
- [19] A. Vlad, S. Yakunin, E. Kolmhofer, V. Kolotovska, L. Muresan, A. Sonnleitner, D. Bauerle, J. D. Pedarnig, Thin Solid Films **518**, 1350 (2009).
- [20] Yumin Kim, Woojin Lee, Dae-Ryong Jung, Jongmin Kim, Seunghoon Nam, Hoechang Kim and Byungwoo Park, Appl. Phys. Lett. **96**, 171902 (2010).
- [21] E. Burstein, Phys. Rev. **93**, 632 (1954).
- [22] Sang-Moo Park, Tomoaki Ikegami, Kenji Ebihara, Paik-Kyun Shin, Appl. Surf. Sci. **253**, 1522 (2006).

---

\*Corresponding author: aurel.pop@phys.ubbcluj.ro